ISTITUTO NAZIONALE DI GEOFISICA E VULCANOLOGIA

ACCEPTED ON ANNALS OF GEOPHYSICS, 62, 2019; Doi: 10.4401/ag-8054

Evaluation of different gravimetric methods to Moho recovery in Iran

Sahar Ebadi [a] (Corresponding author), Riccardo Barzaghi [b], Abdolreza Safari [a], Abbas Bahroudi [c]

[a] School of Surveying and Geospatial Engineering, Research Institute of Geoinformation Technology (RIGT), College of Engineering, University of Tehran, Iran (sahar.ebadi@ut.ac.ir, asafari@ut.ac.ir)
[b] Politecnico di Milano, Department of Civil and Environmental Engineering, Milan, Italy (riccardo.barzaghi@polimi.it)
[c] Exploration department, School of Mining Engineering, University of Tehran, Tehran, Iran (bahroudi@ut.ac.ir)

Evaluation of different gravimetric methods to Moho recovery in Iran

Sahar Ebadi [a] (Corresponding author), Riccardo Barzaghi [b], Abdolreza Safari [a], Abbas Bahroudi [c]

[a] School of Surveying and Geospatial Engineering, Research Institute of Geoinformation Technology (RIGT), College of Engineering, University of Tehran, Iran
(sahar.ebadi@ut.ac.ir, asafari@ut.ac.ir)

[b] Politecnico di Milano, Department of Civil and Environmental Engineering, Milan, Italy
(riccardo.barzaghi@polimi.it)

[c] Exploration department, School of Mining Engineering, University of Tehran, Tehran, Iran
(bahroudi@ut.ac.ir)

Abstract: The complexity of geological units in Iran because of several unique events like tectonics and orogenic activities in this region led to extensive investigations for Moho recovery by seismic methods therein. In this research, three gravimetric methods have been evaluated by some point-wise seismic data. We applied collocation method as an iterative process as well as modified forms of Sjöberg and Jeffrey's theory of isostasy for local Moho depth recovery. The gravity data has been generated by GOCO03S model reduced by topography/bathymetry, sediment and consolidated crust effects. Although the iteration process in collocation approach only slightly changed the estimated depths, this method led to a better agreement with seismic data rather than others. Differences between collocation, Jeffrey and Sjöberg's solutions with seismic studies are similar but Jeffrey and Sjöberg's methods displayed a systematic bias. The standard deviations of the residuals among seismic data and gravimetric solutions are around 6 km. Overall, the evaluation of these approaches indicated that Moho from gravimetric approaches reduced only slightly the standard deviation of seismic Moho estimates. Significant discrepancies with seismic data have been detected in Makran subduction zone, Oman Sea, Persian Gulf and Caspian Sea. The explanation of such inconsistency can be partially due to the poor quality of CRUST1.0 data in these areas, as this model has been used to correct the gravity values that were input in the inversion procedures.

Keywords: Moho, Gravimetric inverse problem, Collocation, Isostasy, Seismic data

1. Introduction

The knowledge of the Mohorovičić discontinuity (Moho) can provide valuable information to understand some topical issues in solid Earth sciences (Sampietro, 2016). Its knowledge in the Iran block is one of the crucial issues in this region. Several unique events like tectonics and orogenic activities in Iran led to a complex geological structure of the area. Thus, it is important to study in deep the peculiar structure of the Iranian Moho applying different methods and different observations in order to have a comprehensive definition of its main features. Moho interface is commonly estimated by either seismic or gravimetric methods. Although seismic Moho estimates have a significant accuracy (at the level of 1-2 km), their coverage over entire of the Earth is quite poor. Thus, in regions where seismic data are sparse or missing, results of gravimetric studies can be profitably used. At global scale, this has been made possible after dedicated gravity-satellite missions, namely the Gravity Recovery and Climate Experiment (GRACE) (Tapley *et al.*, 2004a, Tapley *et al.*, 2004b) and the Gravity field and steady-state Ocean Circulation Explorer (GOCE) (Floberghagen *et al.*, 2011). These two missions have provided global gravity field with an accuracy and a resolution which is suitable for investigating the Moho structure. Among successful seismic estimates, the early results dated back to Beloussov *et al.* (1980). The most widely known crustal model based on seismic refraction is CRUST5.1 model (Mooney *et al.*, 1998). Bassin *et al.* (2000) further upgraded it and called the new version, CRUST2.0. The CRUST1.0 (Laske *et al.*, 2013) including ice layers, water, sediments and consolidated crustal layers, is the most recent version compiled with a 1×1 arc-deg spatial resolution. As already pointed out, because of insufficient seismic data coverage over large areas, gravimetric or combined gravimetric/seismic solutions have been utilized. Based on some isostasy hypotheses on compensating the Earth's topographic masses, gravity data can be used to determine the Moho depth. Several basic theories were suggested to explain the mechanism of isostasy like those proposed by Pratt-Hayford (Pratt, 1855, Hayford, 1909) and Airy-Heiskanen (Airy, 1855, Heiskanen, 1931). Vening Meinesz (1931) modified the Airy-Heiskanen theory by considering a regional instead of a local compensation based on a thin plate lithospheric flexure model (Watts, 2001). Vening Meinesz theory had been modified by Parker (1973) in an iterative approach for Moho determination and Oldenburg (1974) made an attempt to stabilise this method by applying a low-pass filtering technique. The combination of these two methods was known as a Parker-Oldenburg method and it has been generalized for the 3-D gravity inversion by Gómez-Ortiz and Agarwal (2005) and Shin *et al.* (2007). Braitenberg *et al.* (2000) developed a similar method with integration of seismic data; also they estimated

variation of the Moho under the Tibet plateau by an iterative inversion method. Moritz (1990) improved the Vening Meinesz inverse problem for a global compensation by adopting the spherical approximation model of the Earth. Since there were some theoretical deficiencies in this isostatic method, Sjöberg (2009) reformulated Moritz's theory and called it as the Vening Meinesz Moritz (VMM) problem. In this approach he solved a non-linear Fredholm's integral equation of the first kind. Bagherbandi and Sjöberg (2012) made a comparison between the gravimetric VMM and local Airy-Heiskanen methods in the determination of Moho depth. Another approach based on the inversion of gravity data to determining the Moho depth is collocation method (Krarup, 1969, Tscherning, 1985, Moritz, 1990). Barzaghi *et al.* (1992) proposed an approach based on collocation principle, which propagate the covariance structure of the depth interface to the covariance function of the observed gravity field. Barzaghi *et al.* (2015) applied collocation method by combining the global gravity-gradient information of GOCE and local gravity data to Moho recovery. Barzaghi and Biagi (2014) implemented then a further version of the collocation method by including seismic Moho depths as input data. Braitenberg and Ebbing (2009) studied the structure of the crust by combination of GRACE and terrestrial gravity data. Some other scientists made attempt to estimate Moho depth by applying GOCE gravity gradient data (Braitenberg *et al.*, 2010, Sampietro, 2011, Sampietro *et al.*, 2014). Reguzzoni *et al.* (2013) combined seismic and GOCE data to obtain a new global Moho model. Tenzer *et al*. (2009, 2011, 2012a, 2012b) proved that applying the crustal density-contrast stripping corrections is appropriate for a gravimetric Moho recovery. They showed that gravitational contributions of topography and major known crustal density structures have a large spatial correlation with the Moho geometry.

In the area under investigation in this paper, several studies based on seismic data have been performed for the determination of the regional Moho model. Most of these studies concentrated on a specific area, for instance profiles between Shiraz-Mashhad, Tehran-Mashhad and Mashhad-Tabriz (Asudeh, 1982), the southern part of the Caspian Sea (Mangino and Priestley, 1998), Tehran region (Hatzfeld *et al.*, 2003), Mashhad (Doloei and Roberts, 2003, Javan Doloei, 2003), Central Alborz and the northern Iran (Sodoudi *et al.*, 2009, Radjaee *et al.*, 2010), central Zagros (Paul *et al.*, 2006, Shad Manaman *et al.*, 2011), Kopeh-Dagh (Nowrouzi *et al.*, 2007), Naein (Nasrabadi *et al.*, 2008), the northwest Iran (Taghizadeh-Farahmand *et al.*, 2015), and Sanandaj-Sirjan zone (Sadidkhouy *et al.*, 2012). Furthermore, based on terrestrial gravity data in this area with a quite homogenously coverage, Dehghani and Makris (1984) combined gravimetric and seismic data to determination of the crustal

structure of Iran. Abbaszadeh *et al.* (2013) compared the effective elastic thickness of the lithosphere estimated by terrestrial and satellite data in Iran. Eshagh *et al.* (2017) reformulated two isostatic methods for Moho recovery by considering contributions of mean Moho over the whole Moho spectrum.

In this paper, we adopt collocation method as well as two isostatic approaches to determine the Moho depths inverting gravity data over Iran. The collocation inversion method for a two-layer model devised by Barzaghi and Biagi (2014) is applied. In addition, the generalized form of Jeffrey and Sjöberg's method proposed by Eshagh *et al.* (2017) have been utilized in this study. These methods have been applied to gravity from GOCO03S gravitational model (Mayer-Gürr *et al.*, 2012) reduced for the SRTM30_PLUS topographic/bathymetric data (Becker *et al.*, 2009), the sediment and the crystalline data of CRUST1.0 (Laske *et al.*, 2013). Comparisons of these Moho depth estimates have been finally performed with the seismic estimates available from literature.

2. The theoretical background

In this section, we review three gravimetric inversion methods that can be successfully applied to estimate the Moho depth. At first, we describe the procedure based on the collocation principle. Subsequently, we also discuss two alternative isostatic approaches, which are reformulations of Jeffrey and Sjöberg's theories.

2.1 The collocation solution

The collocation method for Moho estimation is based on a stochastic approach derived from the Wiener filtering and prediction theory that allows estimating the signal correlated component based on the covariance structure of the data (Barzaghi and Biagi, 2014). In the years, it has been applied to determine the gravimetric estimate of the Moho (Barzaghi *et al.*, 1992, Barzaghi and Biagi, 2014, Barzaghi *et al.*, 2015). In this context, the covariance structure of the Moho depth is propagated to the covariance of the observed gravity in a simple two-layer model. In order to apply collocation for estimating the Moho depth, we should consider the following linear relationship which holds in planar approximation (Barzaghi and Biagi, 2014):

$$\Delta g\left(x,y,0\right)=G\iint_{R^2}dxdy\Delta\rho\frac{\varepsilon T_0}{\left[T_0^2+d_{xy}^2\right]^{3/2}} \tag{2-1}$$

Δg is the Bouguer gravity anomaly minus its mean, G is the Newton's gravitational constant, T_0 is the mean Moho depth, ε is the Moho depth undulation with respect T_0, $\Delta\rho$ stands for the mean constant density contrast between the two layers and $d_{xy}=\sqrt{x^2+y^2}$.

Also, the following conditions must be fulfilled (Barzaghi and Biagi, 2014):

1) ε is a weak stationary stochastic process, ergodic in the mean and in the covariance

2) The noises in gravity and depth, n_g and n_ε are spatially uncorrelated zero mean signals

3) The cross-correlations between signals and noises are zero

To perform the computation, the gravity auto-covariance and the cross-covariances between gravity and depth are needed, i.e.:

$$C\left(\Delta g_i,\Delta g_j\right)=C_{\Delta g\Delta g}\left(\left|P_i-P_j\right|\right)=C\left(\Delta g_j,\Delta g_i\right) \tag{2-2}$$

$$C\left(e_i,\Delta g_j\right)=C_{e\Delta g}\left(\left|P_i-P_j\right|\right)=C\left(\Delta g_j,e_i\right) \tag{2-3}$$

Assuming that the observed gravity values contain a noise component, we can write:

$$\Delta g_{OBS}=\Delta g+n_g \tag{2-4}$$

The collocation estimate of ε is (Moritz, 1980, Barzaghi *et al.*, 1992, Barzaghi and Biagi, 2014):

$$\hat{e}=\left[c_{e\Delta g}^T\right]C_{ll}^{-1}l \tag{2-5}$$

With

$c_{e\Delta g_i}=C\left(e_k,\Delta g_i\right)$, $l=\left[\Delta g_{OBS}\right]$ and $C_{ll}=\left[C_{\Delta g_{OBS}\Delta g_{OBS}}\right]$.

As the first step to use this approach, the empirical covariance function of Δg_{OBS} should be estimated and modelled with appropriate positive definite model functions (Moritz, 1980). Under the hypotheses previously stated, the empirical covariance can be estimated as (Barzaghi *et al.*, 1992):

$$\hat{C}_{\Delta g \Delta g}(\Delta P_k) = \frac{1}{N}\sum_{i=1}^{N}\frac{1}{N_i}\sum_{j=1}^{N_j}\Delta g_{OBS}(Q_i)\Delta g_{OBS}(Q_j)$$
$$P_{k-1} < |Q_i - Q_j| < P_k, \qquad \Delta P_k = P_k - P_{k-1} \tag{2-6}$$

Also, auto and cross-covariance models must be defined in order to derive the estimator of ε for Moho determination. One possible model for the auto covariance of Δg (see Barzaghi and Biagi (2014)) is:

$$C_{\Delta g \Delta g}(r) = \frac{A J_1(ax)}{ax} \tag{2-7}$$

Where $J_1(.)$ is the first order Bessel function.

If this auto-covariance is considered, one can prove (Barzaghi *et al.*, 1992) that:

$$C_{\varepsilon \Delta g}(P,Q) = \frac{A}{2\pi G \bar{\rho} \alpha}\int_0^{\alpha} dk k e^{k\bar{H}} J_0(k|P-Q|) \tag{2-8}$$

which can be evaluated by numerical integration methods.

The parameters A and α are determined so that the model (2-7) fits the empirical estimated covariance values of Δg. After deriving $C_{\varepsilon \Delta g}(P,Q)$ by the expression above, we can then obtain ε by applying formula (2-5). The final Moho estimate is then given as $T = T_0 + \varepsilon$.

Also, in order to refine the estimate, iterations on gravity residuals can be performed so that the final solution is obtained as $T = T_0 + \varepsilon_1 + \ldots + \varepsilon_n$. Usually two or three iterations are computed.

2.2 The Jeffrey's solution

Jeffrey (1976) has solved the problem of isostasy for Moho modelling in a very similar way to the VMM method (Sjöberg, 2009). Eshagh and Hussain (2016) proposed a different modelling of the isostatic gravity disturbance δg^{I} by considering the gravitational effects of topography and bathymetry, sediments and consolidated crystalline basement as follows:

$$\delta g^{\mathrm{I}} = \delta g - \delta g^{\mathrm{TB}} - \delta g^{\mathrm{S}} - \delta g^{\mathrm{Crys}} + \delta g_{\mathrm{C}} \tag{2-9}$$

In this equation, δg denotes the observed gravity disturbance which is the difference between measured and normal gravity at a computation point on the Earth, δg_{C} is the compensation attraction, δg^{TB} is the topographic/bathymetric effect on δg, δg^{S} and δg^{Crys} represent the gravitational effects of sediment and consolidated crust, respectively. Moritz (1990) and Sjöberg (2009) applied this equation as a fundamental condition to solve the VMM problem. In order to define the compensation potential in equation (2-10), Eshagh *et al.* (2017) arranged the formula in Jeffrey (1976) in the following way:

$$V_{\mathrm{C}} = G\iint_{\sigma}\int_{R-T_0-\varepsilon}^{R-T_0}\frac{\Delta\rho r'^2}{l}\mathrm{d}r'\mathrm{d}\sigma = G\iint_{\sigma}\sum_{n=0}^{\infty}\frac{\Delta\rho}{r^{n+1}}\int_{R-T_0-\varepsilon}^{R-T_0} r'^{n+2}\mathrm{d}r' P_n(\cos\psi)\,\mathrm{d}\sigma \tag{2-10}$$

As stated before, ε is the variation of the Moho depths relative to the mean value indicated by T_0. In this equation, R is the radius of the Earth, σ is the unit sphere, r' denotes the geocentric distance of the infinitesimal mass element while $\mathrm{d}r'$ and $\mathrm{d}\sigma = \sin\theta\mathrm{d}\theta\mathrm{d}\lambda$ are the radial and the surface integration elements, $P_n(\cos\psi)$ is the Legendre polynomial of degree n for the argument of the geocentric angle ψ. θ and λ represent the spherical co-latitude and longitude of the element, l is the Euclidean spatial distance which is a function of the r' (see. Heiskanen and Moritz (1967)).

Further, Eshagh *et al.* (2017) solved the radial integral and expanded δg_{C} in a spectral form according to the Heiskanen and Moritz (1967) scheme:

$$\delta g_{\mathrm{C}}\Big|_{r=R} = GR\iint_{\sigma}\Delta\rho\sum_{n=0}^{\infty}\frac{n+1}{n+3}\kappa^{n+3}\left[1-\left(1-\frac{\varepsilon}{R-T_0}\right)^{n+3}\right]P_n(\cos\psi)\,\mathrm{d}\sigma \tag{2-11}$$

Where $\kappa = 1-\dfrac{T_0}{R}$.

Also Eshagh *et al.* (2017) approximated the term $[\varepsilon/(R\text{-}T_0)]^{n+3}$ by a binomial series and after simplification, (2-11) reduces to:

$$\delta g_{\mathrm{C}} = \frac{GR}{R-T_0}\sum_{n=0}^{\infty}(n+1)\kappa^{n+3}\iint_{\sigma}(\Delta\rho\varepsilon)P_n(\cos\psi)\,\mathrm{d}\sigma \tag{2-12}$$

They wrote this equation according to Laplacian harmonics of $\Delta\rho\varepsilon$:

$$\delta g_{\mathrm{C},n} = 4\pi G\frac{n+1}{2n+1}\kappa^{n+2}(\Delta\rho\varepsilon)_n \tag{2-13}$$

By considering Eq. (2-9) and inserting (2-13) into that, they got:

$$(\Delta\rho\varepsilon)_n = -\frac{1}{4\pi G}\frac{2n+1}{n+1}\kappa^{-(n+2)}\left(\delta g_n - \delta g_n^{\mathrm{TB}} - \delta g_n^{\mathrm{S}} - \delta g_n^{\mathrm{Crys}}\right) \tag{2-14}$$

Eshagh *et al.* (2017) took the summation from both sides of Eq. (2-14) and extract ε from the resulting expression and finally arrived at:

$$\varepsilon = -\frac{1}{4\pi G\Delta\rho}\sum_{n=0}^{\infty}\frac{2n+1}{n+1}\kappa^{-(n+2)}\left(\delta g_n - \delta g_n^{\mathrm{TB}} - \delta g_n^{\mathrm{S}} - \delta g_n^{\mathrm{Crys}}\right) \tag{2-15}$$

Since ε is the undulation of Moho depths with respect to T_0, the total Moho depth is given as $T = T_0 + \varepsilon$.

2.3 The Sjöberg's solution

The Vening Meinesz Moritz (VMM) inverse problem of isostasy (Sjöberg, 2009) has been developed and applied successfully over different areas of the Earth. The main difference between Jeffrey and Sjöberg's method is how to write the compensation potential. Sjöberg (2009) used the compensation potential V_{C} derived by Moritz (1990):

$$V_{\mathrm{C}} = G\Delta\rho\iint_{\sigma}\sum_{n=0}^{\infty}\frac{1}{r^{n+1}}P_n(\cos\psi)\left\{\int_{R-T}^{R} r'^{n+2}\mathrm{d}r' - \int_{R-T_0}^{R} r'^{n+2}\mathrm{d}r'\right\}\mathrm{d}\sigma \tag{2-16}$$

Eshagh *et al.* (2017) solved the integrations by assuming $T = T_0$ and obtained the compensation attraction of the gravity disturbance as follows:

$$\begin{aligned}\delta g_{\mathrm{C}} = {} & GR\Delta\rho\iint_{\sigma}\sum_{n=0}^{\infty}(n+1)\frac{T}{R}\left(1-(n+2)\frac{T}{2R}\right)P_n(\cos\psi)\,\mathrm{d}\sigma - \\ & - GR\Delta\rho\iint_{\sigma}\sum_{n=0}^{\infty}\frac{(n+1)}{(n+3)}\left[1-\kappa^{n+3}\right]P_n(\cos\psi)\,\mathrm{d}\sigma\end{aligned} \tag{2-17}$$

Furthermore, they considered the spectral form of δg_{C} and got:

$$\delta g_{\mathrm{C},n} = 4\pi G\Delta\rho\beta_n\frac{n+1}{2n+1}T_n - \frac{4\pi GR\Delta\rho}{3}\left(1-\kappa^{n+3}\right)\delta_{n0} \tag{2-18}$$

Where $\beta_n = 1-(n+2)\frac{T_0}{2R}$.

They proved by inserting Eq. (2-18) into (2-9) that the Moho depth can be obtained as:

$$T = A_{C0} + \frac{1}{4\pi G\Delta\rho}\sum_{n=0}^{\infty}\frac{2n+1}{n+1}\beta_n^{-1}\left(\delta g_n^{TB} + \delta g_n^{S} + \delta g_n^{Crys} - \delta g_n\right) \quad (2\text{-}19)$$

Where $A_{C0} = \frac{R}{3}\left(1-\kappa^3\right)\left(\frac{R}{R-T_0}\right)$. As it can be seen in Eq. (2-19), T_0, besides the zero-degree term, affects all frequencies.

3. The Iran case study

In this section, we present the Iran case study and the application of the three methods previously described to the gravimetric estimate of the Moho in Iran. We divide this section into four parts. In section 3.1 we present a brief geological structure of the area. The used gravity data are described in section 3.2 while in section 3.3 the local gravity Moho estimates over the study area by collocation, the Jeffrey and Sjöberg methods are presented. Finally, in section 3.4 comparisons among different gravimetric and seismic derived Moho values are shown.

3.1 The study area

All methodologies have been applied in Iran over an area limited by the parallels 20° and 45° North and the meridians 40° and 65° East (see Fig. 1). Several unique events like tectonics and orogenic activities led to complicated structural units in this area. By considering the geological features of Iran, some models and interpretations have been proposed for this region (Nabavi, 1976, Eftekharnezhad, 1980, Alavi-Naini, 1993, Aghanabati, 2004, Ghorbani, 2013). According to these studies, a geological setting of this area showing a geological classification of various structural zones of Iran has been devised and is presented in Fig. 1, superimposed on the regional topography. Topography/bathymetric heights were generated by the SRTM30_PLUS model to degree and order 2160 with a resolution of 5'×5' over the study area (Becker *et al.*, 2009). As seen in Fig. 1, the ranges of topography vary from -3182 to 4142 m. Significant topography is seen over the Alborz and Zagros mountains which continues from West-North until East-South. Most of Iran is surrounded by a rough topography except for southern border of Caspian Sea, Central Iran, Lut Block, Jazmourian and Makran basins.

The convergence of the Arabia-Eurasia plate led to the complex features in the Iranian crust and lithospheric mantle. The closure of Tethys Ocean and collision of Arabian-Eurasian plates caused the formation of Iranian plateau during the Mesozoic and Cenozoic period (Berberian and King, 1981, Berberian *et al.*, 1982). Some active and young tectonic structures consist of the collision zones in Zagros, Alborz, Kopeh-Dagh and subduction zones in the Makran and South Caspian Basin were formed as a result of the Arabia-Eurasia convergence (Shad Manaman *et al.*, 2011). This convergence led to formation of the two tectonometamorphic and magmatic belts of Sanandaj-Sirjan zone and the Urumieh-Dokhtar magmatic assemblage.

Central Iran is a triangle located in the middle and bordered by the Alborz Mountains in the North, Lut Block in the East and Urumieh-Dokhtar in the South. In this zone, there are rocks of all ages, from Precambrian to Quaternary, and several episodes of orogeny, metamorphism and magmatism. Sanandaj-Sirjan is located to the South-West of Central Iran and the North-East of Zagros Mountains. A remarkable feature of this zone is the presence of immense volumes of magmatic and metamorphic rocks of Paleozoic and Mesozoic eras. Zagros ranges separate the Arabian Block from the rest of Eurasian tectonic plate. In this area, there are no abundant outcrops of Paleozoic rocks and the area is without magmatic and metamorphic events. Alborz range is located in North of Iran, parallel to the Southern margin of Caspian Sea. This mountain is characterized by different sedimentary rocks. The Kopeh-Dagh Mountains and basin consist largely of extrusive igneous rocks belong to Paleogene volcanic areas. Makran is separated from Jazmourian depression by a long range of ophiolites extending from West to East (cf. Ghorbani (2013)).

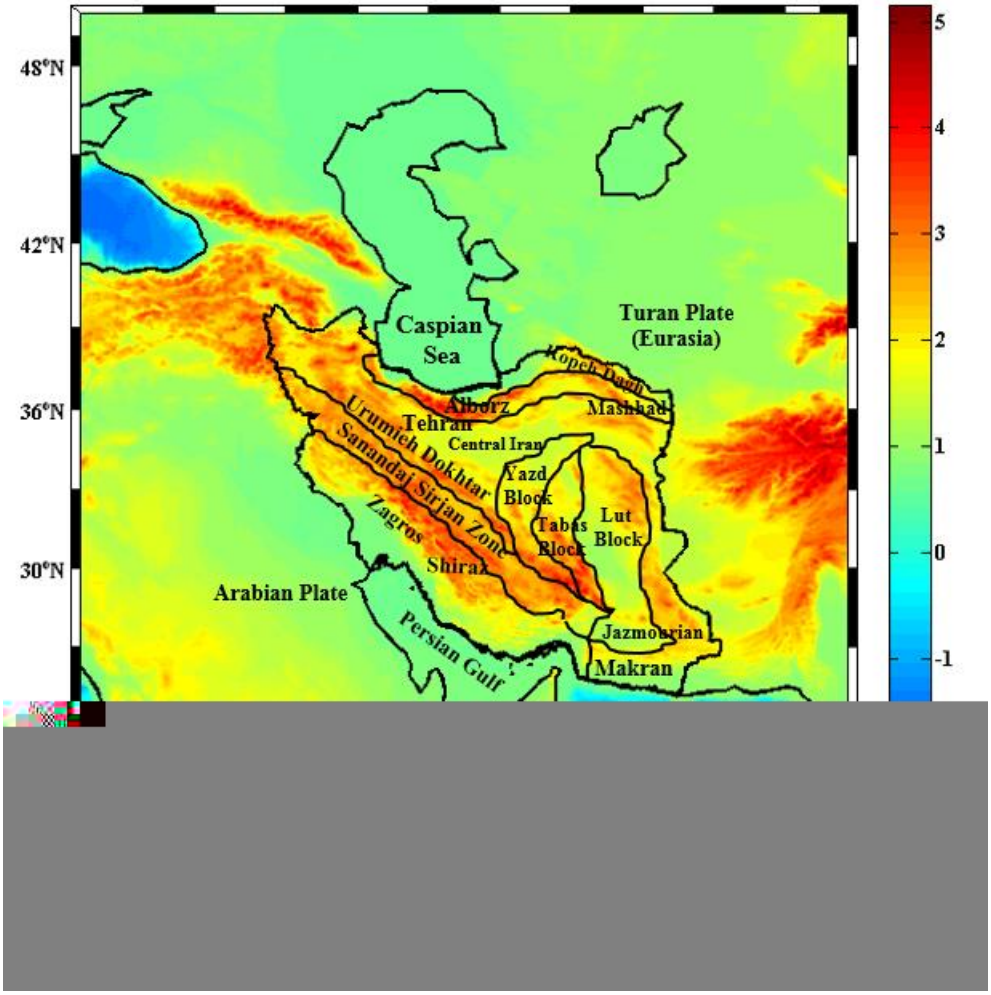

Fig. 1 Topography heights and geological setting of the study area of Iran [km]

3.2 The gravity data set

In this study, the considered gravity data have been synthetized from the GOCO03S gravitational model up to degree and order 180 and were computed on a 0.5×0.5 arc-deg surface grid. In order to obtain the topography/bathymetry (TB) corrections, we applied the spherical harmonics expansion of digital elevation model from SRTM30_PLUS to degree and order 180 consistent with the resolution of CRUST1.0 model. Moreover, for computing the gravity corrections due to sediment and consolidated crustal layers, we used the Earth's crustal model CRUST1.0, which in this area gives mean densities values for the sediments and the consolidated crustal layers that are, respectively, 2060 kg m^{-3} and 2670 kg m^{-3} (see Fig. 2b and 2c). By applying all these corrections we obtained the gravity data that were used in the inversion procedures. Fig. 2d represents the map of the refined Bouguer gravity, in unit of mGal, reduced for the gravitational contribution of crustal density heterogeneities over the

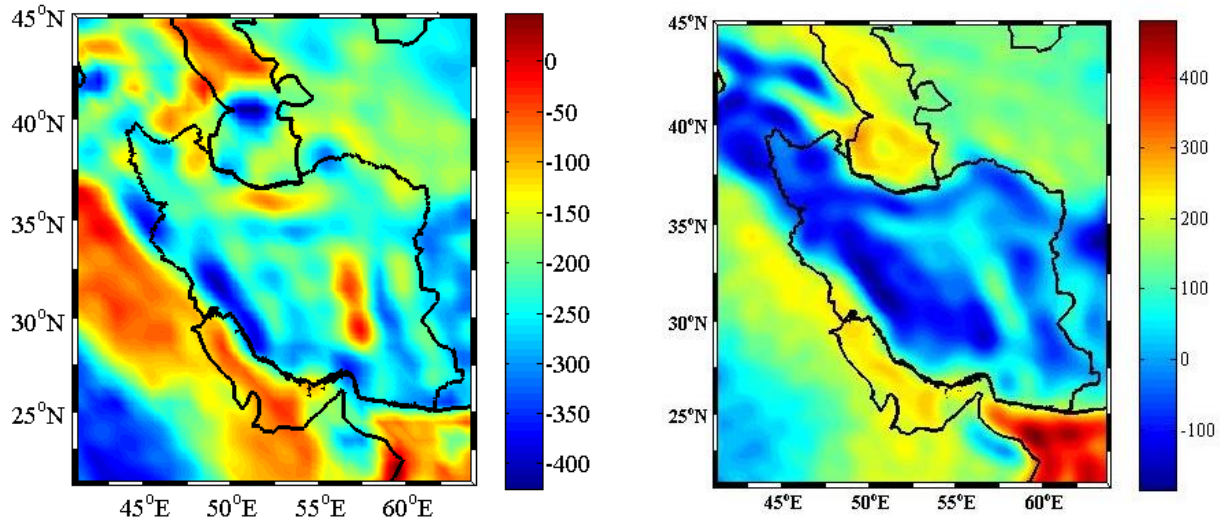

Fig. 2 a) the TB gravitational effect; b) the gravitational effect of sediments; c) the gravitational effect of consolidated crust; d) the reduced Bouguer gravity anomalies [mGal].

3.3 The gravimetric Moho estimates

The three methods described in section 2 for determination of Moho were applied in the study area. The computations were accomplished by setting $T_0 = 44$ km, which is the mean of depths estimated from seismic studies (Mangino and Priestley, 1998, Paul *et al.*, 2006, Taghizadeh-Farahmand *et al.*, 2010, Radjaee *et al.*, 2010, Tatar and Nasrabadi, 2013, Taghizadeh-Farahmand *et al.*, 2015, Motaghi *et al.*, 2015, Abdollahi *et al.*, 2018).

As stated above, the collocation approach in planar approximation has been applied to GOCE derived reduced Bouguer gravity, i.e. Bouguer gravity anomalies reduced for sediment and consolidated crust effects. Moho depths have been determined with respect to mean value T_0 while the ε values have been obtained according to the scheme described in section 2. In this computation, the constant density contrast between crust and mantle has been set to 600 kg m^{-3}. The gravity data, obtained by applying combined topography/bathymetry gravitational effect from SRTM30_PLUS data and corrections for the sediment and consolidated crust data generated from the CRUST1.0, has been re-gridded on a regular (x,y) grid in the investigation area (see Fig. 3):

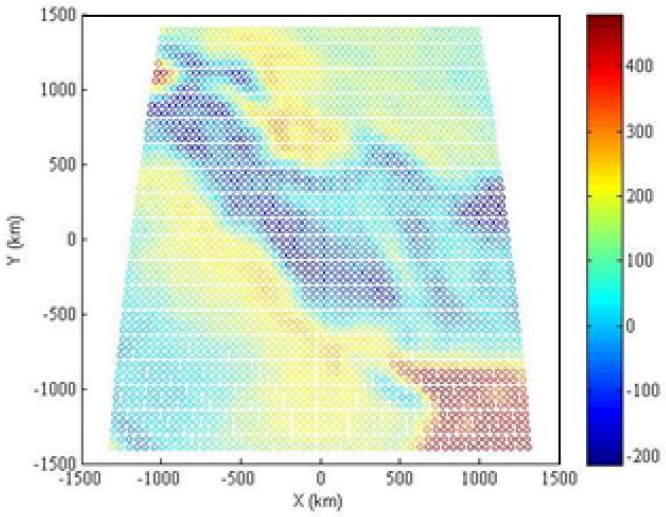

Fig. 3 Bouguer gravity anomaly reduced by topography/bathymetry, sediment and consolidated crust corrections on a (x,y) grid [mGal]

The collocation procedure has been then applied iteratively. The behaviour of the empirical covariance function of gravity data and the best-fit model with the related parameters can be seen in Fig. 4 for the three steps that have been performed to get the final estimate.

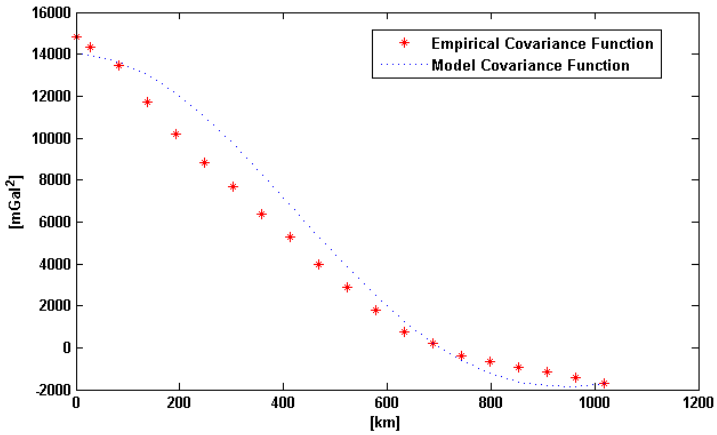

a) First step: $\hat{A}_{\delta g}$ = 14000 mGal^2, $\hat{\alpha}$ = 0.0055 km^{-1}, $\hat{\sigma}_n^2$ = 815 mGal^2

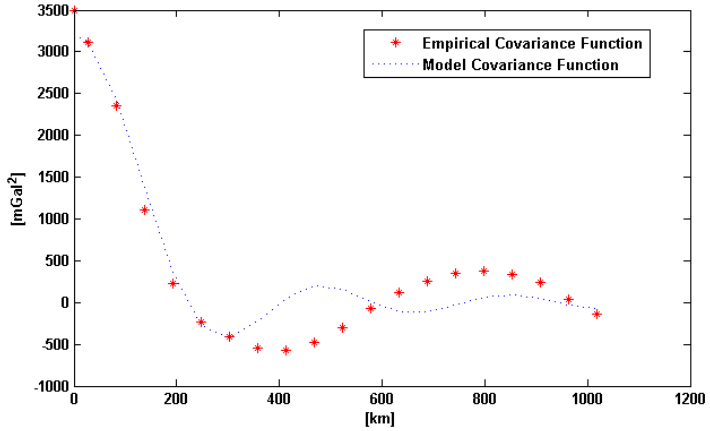

b) Second step: $\hat{A}_{\delta g}$ = 3200 mGal^2, $\hat{\alpha}$ = 0.0135 km^{-1}, $\hat{\sigma}_n^2$ = 290 mGal^2

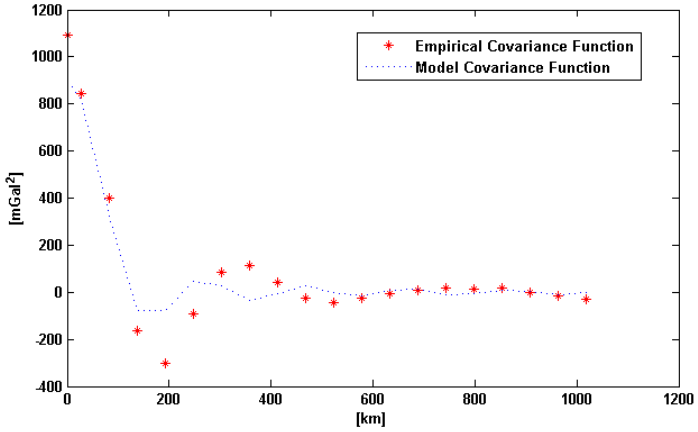

c) Third step: $\hat{A}_{\delta g}$ = 900 mGal^2, $\hat{\alpha}$ = 0.0317 km^{-1}, $\hat{\sigma}_n^2$ = 192 mGal^2

Fig. 4 The empirical covariance function of the gravity data and the best-fit model

In this figure, parameter A is the covariance value in the origin, α is the scaling factor for argument of Bessel function and $\hat{\sigma}_n^2$ is the noise variance, i.e. the difference between the empirical value and the model function at the origin. A and α are found by letting the first empirical zero coincide with the zero of the model function and assuming the model function coincide with the empirical one at the second point (Barzaghi *et al.*, 1992). In the first step, the model function which best described the empirical values is J_1 Bessel function divided by its argument, with A=14000 mGal^2 and parameter $\hat{\alpha}$ =0.0055 km^{-1}. A value is sufficiently close to initial one of empirical function, which is 14815 mGal^2. The difference between the two values in the origin, i.e. the noise variance, has been fixed to 815 mGal^2. In the second step, residuals of gravity from the first inversion step have been used as input data. As can be

seen in Fig. 4 the variance of these residuals, i.e. the value in the origin of the empirical function, decreased drastically to 3490 mGal^2 and the signal variance, i.e. the A value, has been set to 3200 mGal^2. The $\hat{\alpha}$ and $\hat{\sigma}_n^2$ quantities have been fixed at 0.0135 km^{-1} and 290 mGal^2, respectively. Furthermore, in third step, based on the residual gravity from the second iteration, model covariance parameters were fixed at $\hat{A}_{\delta g}$ = 900 mGal^2, $\hat{\alpha}$ = 0.0317 km^{-1}, $\hat{\sigma}_n^2$ = 192 mGal^2. This iterative process has been stopped at the third iteration since the covariance function of the third step residuals has a correlation length (the distance at which the covariance function is half of its value in the origin) that is comparable with the grid step. Results of this procedure are shown in Fig. 5 and related statistics are summarized in Table 2.

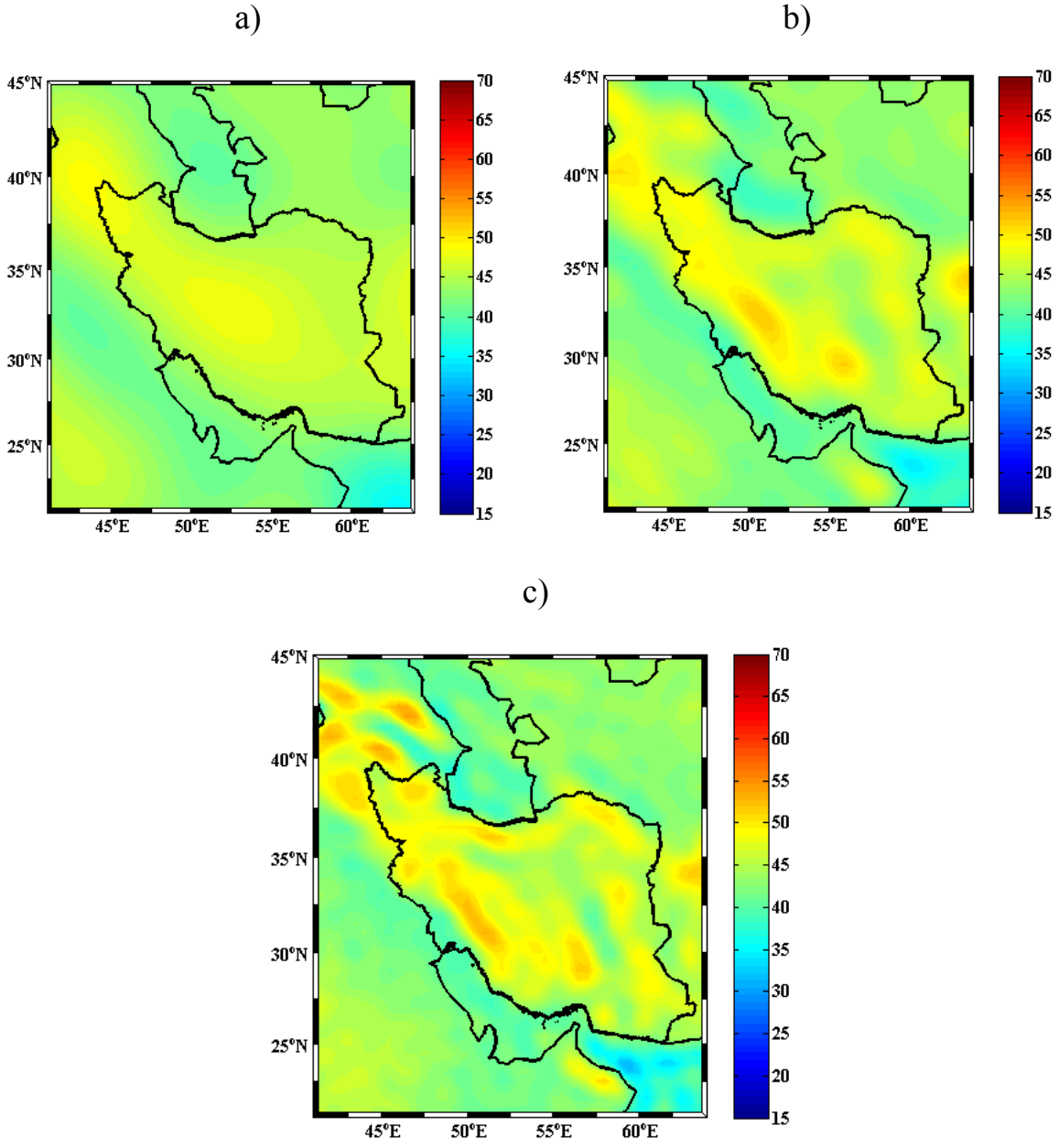

Fig. 5 Map of Moho model derived from collocation method in a) First step b) Second

step c) Third step [km]

Table. 2. Statistics of Moho depth computed according to the collocation method [km]

	Step	Max	Mean	Min	STD
Collocation Method	First step	49.0	44.0	35.5	2.4
	Second step	51.9	44.0	32.8	3.0
	Third step	54.6	44.0	31.6	3.4

The final estimate (see Fig. 5c), obtained by adding the e_i values coming from the iterative procedure to the mean depth $T_0 = 44$ km, shows maximum depths under the Zagros Mountain, the Sanandaj-Sirjan and the Urumieh-Dokhtar belts with spread under the Alborz Mountain and Kopeh-Dagh, while the minimum depth is under the Oman Sea and the border of Caspian. In first step it can be observed that the Moho depth varies between 35.5 km and 49.0 km and in most areas, depth of Moho is below 40 km. In second step, statistics are similar to previous with a slight increase of the standard deviation of the estimated Moho depths. As seen in Fig. 5c the Moho depths coming from the third step are more high frequency (standard deviation increases to 3.4 km) and ranges between 31.6 km and 54.6 km.

Based on gravity disturbance data, coming from the GOCO03S, completed to degree and order 180, we then estimated the Moho depth over Iran with the gravimetric approaches devised by Sjöberg and Jeffrey. As done in the collocation solution, the mean Moho depth has been set to 44 km. Also, the constant density contrast between crust and mantle has been set to 600 kg m^{-3} and corrections including topography/bathymetry, sediment and consolidated crust has been accounted as well. The results are plotted in Fig. 6 and the summary of statistics is given in Table. 3. These solutions show a similar pattern with a large Moho depth under Zagros and Alborz mountains and also along Sanandaj-Sirjan and Urumieh-Dokhtar belts and Kopeh-Dagh. The areas with minimum depth are under the Oman Sea, some parts of Caspian and Persian Gulf while central Iran, Tabas and Lut block have relatively shallow Moho depth. As seen in Fig. 6, Sjöberg method gives a smoother solution than the one based on Jeffrey method.

Minimum Moho depths in both these methods are lower than minimum depths estimated using the collocation method. Statistics in Table. 3 show a minimum Moho depth of 17.6 km and 33.9 km for Jeffrey and Sjöberg methods, respectively. Also, the maximum Moho depth

according to Jeffrey solution seems to be overestimated since this method has given a depth around 67.4 km near the northwest of Iran. On the contrary, by applying the Sjöberg method, the maximum Moho depth in Iran has been estimated to 59.6 km.

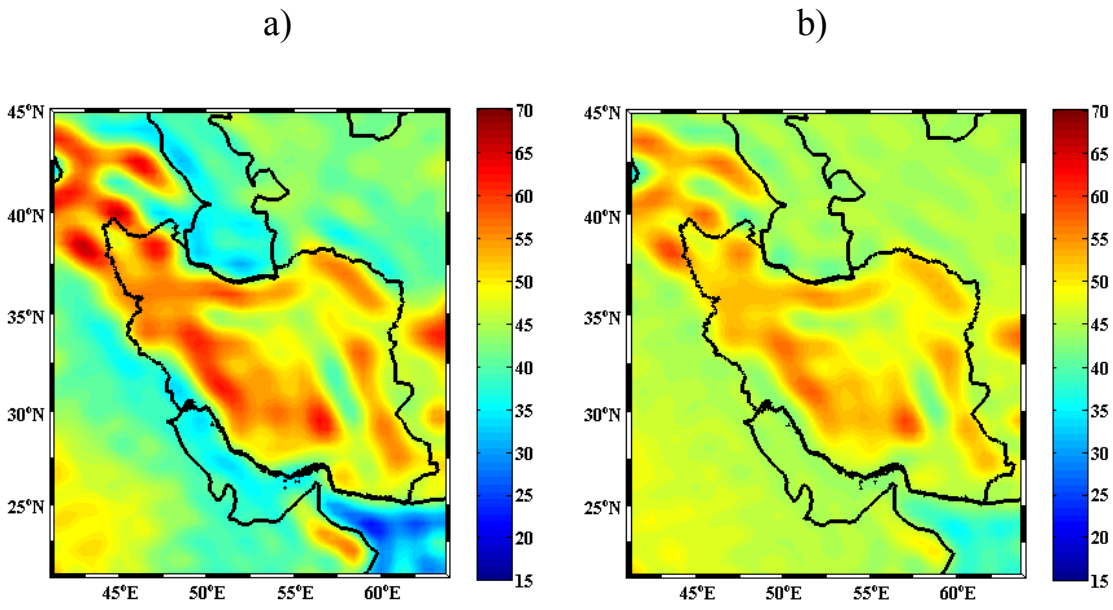

Fig. 6 Map of Moho model derived from a) Jeffrey's method b) Sjöberg's method [km]

Table. 3. Statistics of Moho depth computed according to Jeffrey and Sjöberg's method [km]

	Max	Mean	Min	STD
Jeffrey	67.4	44.9	17.6	7.2
Sjöberg	59.6	46.6	33.9	3.7

3.4 Comparing gravimetric and seismic Moho estimates

To validate the gravimetric Moho solutions, we compared them with existing regional seismic studies for Iran (Mangino and Priestley, 1998, Paul *et al.*, 2006, Taghizadeh-Farahmand *et al.*, 2010, Radjaee *et al.*, 2010, Tatar and Nasrabadi, 2013, Taghizadeh-Farahmand *et al.*, 2015, Motaghi *et al.*, 2015, Abdollahi *et al.*, 2018). A compilation of these numerous seismic datasets has been prepared and checks for their consistency were performed. In this way, we defined a selected collection of seismic Moho values in the Iran area, which consists of 277 points. These models are shown in Fig. 7 and their statistics are given in Table 4. The maximum Moho depth is located under the Sanandaj-Sirjan zone and surrounding mountains.

By seismic estimates, the minimum depth of Moho is under the Oman Sea and Makran subduction zone. As it can be seen, Moho depths derived from seismic studies varies between 18.5 km and 66 km.

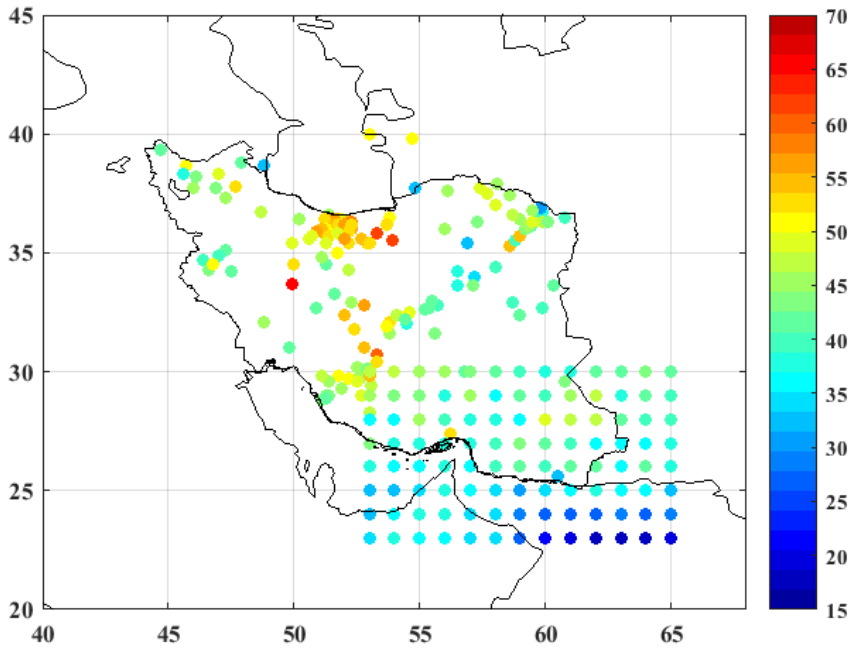

Fig. 7 Moho derived from seismic results [km]

Table. 4 Statistics of Moho depth from Seismic estimates [km]

	Max	Mean	Min	STD
Seismic data	66.0	44.0	18.5	8.2

These seismic values were then compared with the gravity derived estimates. In order to perform the comparison, we interpolated the gridded gravity estimates on the sparse seismic point using linear interpolation.

The differences are plotted in Fig. 8 and the statistics of the differences are summarized in Table. 5. As one can see in Fig. 8a, the differences between the collocation solution and seismic data are between -17 km and 21.9 km. The differences between Jeffrey's and Sjöberg's solutions and seismic data range from -11.1 km to 22.2 km and -10.8 km to 23.4 km, respectively (see Fig. 8b and 8c).

a)

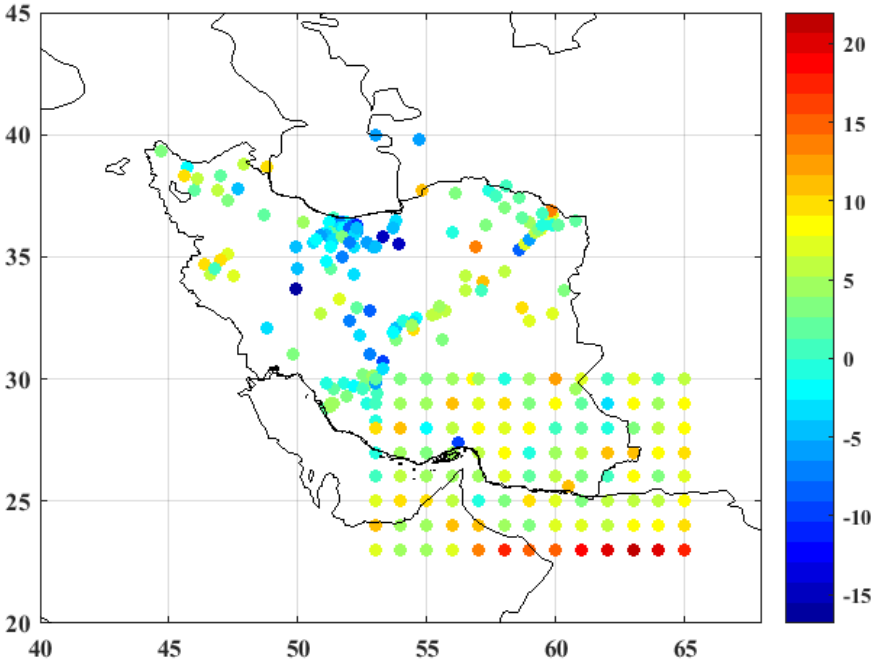
45
40
35
30
25
20
40
45
50
55
60
65
20
15
10
5
0
-5
-10
-15

b)

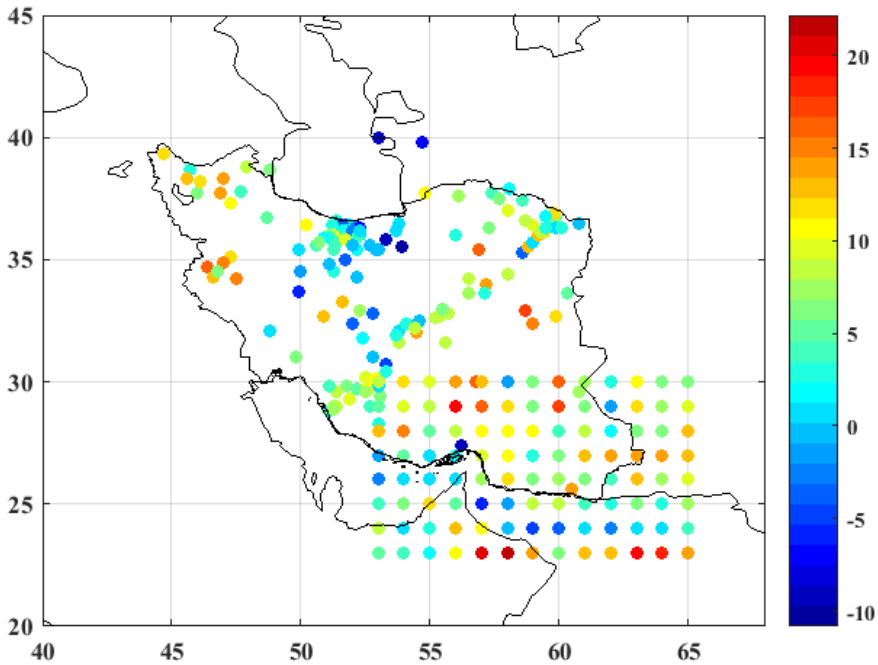
45
40
35
30
25
20
40
45
50
55
60
65
20
15
10
5
0
-5
-10

c)

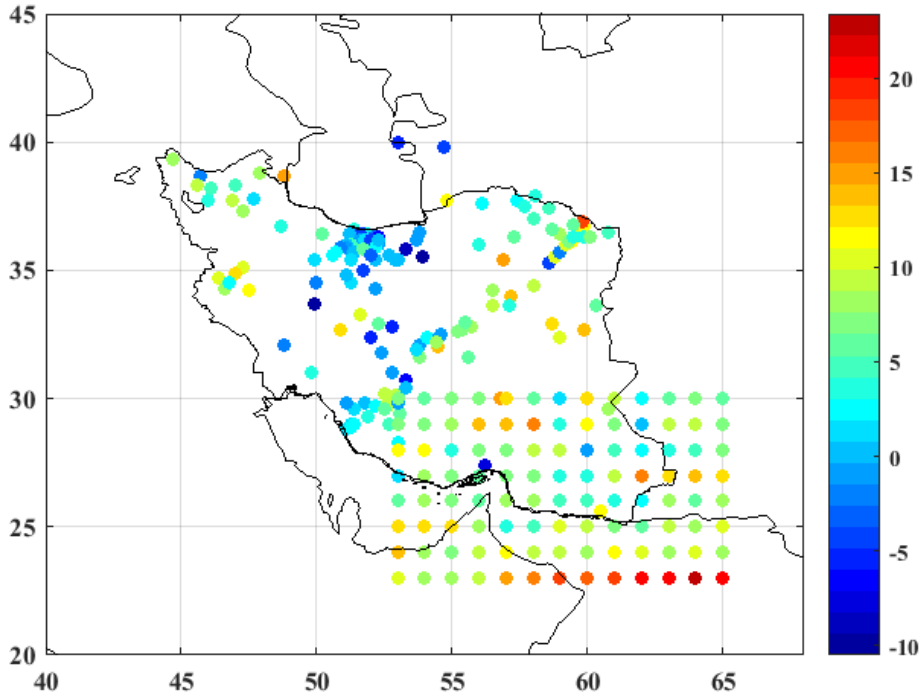

Fig. 8 Differences between seismic data and Moho derived from a) Collocation method b) Jeffrey's method c) Sjöberg's method [km]

Table. 5. Statistics of differences between gravimetric Moho estimates and seismic results [km]

	Max	Mean	Min	STD	RMS
Collocation Method	21.9	2.4	-17.0	**6.3**	**6.7**
Jeffrey Method	22.2	5.7	-11.1	**6.1**	**8.3**
Sjöberg Method	23.4	5.2	-10.8	**6.0**	**7.9**

As it can be seen in Table 5, the STDs of the differences with respect to seismic data are around 6 km, the smaller STD values being obtained by the Sjöberg estimate. Since the STD

of seismic data 8.2 km (see Table 4), we can conclude that the gravimetric Moho estimates are not so highly correlated with the seismic estimates. Furthermore, the statistics show that Jeffrey and Sjöberg's method give estimated Moho values that have biases with respect to the seismic values larger than collocation. This reflects in the RMSs values that show how collocation gives a Moho estimate which is, overall, closer to the seismic values.

This overall analysis can be further specified for different sub-areas in the Iran region where existing regional seismic solutions are available.

Central Zagros and specifically Sanandaj-Sirjan zone are regions where the maximum depth of Moho has been revealed therein. According to our computations, collocation solution indicated a 55 km Moho depth for this area. Sjöberg and Jeffrey's methods also indicated Moho depths at the level of 55 km and 60 km for this zone, respectively. Dehghani and Makris (1984) by using integrated gravity and seismic data estimated a crustal thickness beneath the central Zagros in 55 km, which fully agrees with the results of collocation and Sjöberg's methods. Hatzfeld *et al.* (2003) proposed a depth of 46 km for the crustal thickness at the single station close to the town of Ghir in central Zagros.

Another investigation of the lithospheric structure of the Iranian Plateau has been performed by Asudeh (1982) along three profiles connecting Mashhad to Shiraz, Tehran to Mashhad and Shiraz to Tabriz. He reported crustal thickness along these profiles 43, 45 and 46 km, respectively. Doloei and Roberts (2003) and Javan Doloei and Ghafory-Ashtiany (2004) have proposed 52 km for depth of Moho in Mashhad. By collocation solution, depth of Moho in Mashhad has been estimated in about 52 km which is in agreement with Javan Doloei (2003) and Javan Doloei and Ghafory-Ashtiany (2004) results. Also, Sjöberg and Jeffrey's method estimated the Moho depth of about 52 and 56 km in Mashhad, respectively. Doloei and Roberts (2003) used seismic data and suggested a crustal thickness of 46 km in Tehran located southern part of the central Alborz. Results of collocation, Sjöberg and Jeffrey's method gave values of Moho depths of 43, 45 and 47 km in Tehran, respectively.

Dehghani and Makris (1984) showed that the crustal thickness varies from 35 km beneath Alborz Mountains to 54 km in central Alborz. Sobouti and Arkani-Hamed (1996) identified a 45 km crustal thickness along the Alborz Mountains. In the analysis of 290 teleseimic events carried out by Sodoudi *et al.* (2009) at 12 short-period stations of the Tehran telemetric network, an average depth of 44-46 km for Moho under central Alborz has been estimated. Radjaee *et al.* (2010) reported the crustal thickness 48 km under the northern part of the central Iranian Plateau. Also, they found a variable crustal thickening between 55 and 58 km under central Alborz. Shad Manaman *et al.* (2011) estimated a thick Moho with 55-60 km

depth beneath the central Alborz. Jiménez-Munt *et al.* (2012) and Taghizadeh-Farahmand *et al.* (2015) estimated crustal thickness 50 and 54 km in central Alborz, respectively. The results of collocation and Sjöberg's method indicated depth of Moho in that area around 53 km which is close to the values reported by Dehghani and Makris (1984), Radjaee *et al.* (2010) and Shad Manaman *et al.* (2011). The estimation of Jeffrey's method has given a quite overestimated depth of 60 km in this area.

Paul *et al.* (2006) estimated crustal thickness beneath Urumieh-Dokhtar magmatic area around 42 km. Nasrabadi *et al.* (2008) indicated that Moho depth is 40 km beneath Maku station in northwest of Iran. Taghizadeh-Farahmand *et al.* (2010) applied P and S seismic waves to recover the crustal thickness around 48 km in this area. According to Taghizadeh-Farahmand *et al.* (2015), the average of Moho depth varies from 41 km in the northwest Iran to 45-49 km in the northeast. Jiménez-Munt *et al.* (2012) estimated the crustal structure from combination of the geoid height and elevation data with thermal analysis. Their results showed the crustal thickness of 50 km beneath the Alborz and Kopeh-Dagh mountains. By our gravimetric solutions depth of Moho in Kopeh-Dagh has been estimated slightly more than 50 km.

Mangino and Priestley (1998) estimated the Moho depth at 30-33 km beneath the South Caspian Basin. Also, Shad Manaman *et al.* (2011) estimated similar values for Moho depth in this area. Our results from gravimetric methods there indicate the Moho depth of about 37, 38 and 33 km by collocation, Sjöberg and Jeffrey's methods, respectively.

Shad Manaman *et al.* (2011) investigated the Moho depth through the Makran subduction zone and reported values around 25-30 km for the Oman seafloor and Makran. Taghizadeh-Farahmand *et al.* (2015) presented a depth of 35 km over this area. Abdollahi *et al.* (2018) reported range of Moho from 18 to 28 km in Oman Sea. The collocation solution gave the Moho depth at around 33 km in Oman Sea. Also, results of Jeffrey and Sjöberg's methods has led to depth values of 20 and 34 km in this area, respectively. Our estimations by collocation and Sjöberg's method are different from the results of seismic studies at the subduction zone and the tectonic border in the Oman Sea. This could be related to the procedure that we adopted for correcting the gravity values. Indeed, Eshagh *et al.* (2017) concluded that the sediment and crystalline corrections computed using the CRUST1.0 have a low quality in oceanic areas.

Dehghani and Makris (1984) reported that the crustal thickness varies between 45 and 48 km in the eastern Iran. Nowrouzi *et al.* (2007) estimated depth of Moho around 44-50 km under Kopeh-Dagh. Jiménez-Munt *et al.* (2012) suggested Moho depth minima of about 36 km beneath the Lut block. According to Shad Manaman *et al.* (2011), Moho depth varies from 35

km to 40 km in central Iran and Lut block. Nasrabadi *et al.* (2008) mentioned that the crustal thickness deepens up to 56 km under the Naein station in central Iran. The results of Sadidkhouy *et al.* (2012) showed that depth of Moho in Isfahan area is variable between 38.5 and 43 km. Our solutions by gravimetric methods give the Moho depth ranging from 47 km in central Iran to 44 km in Lut block, which is in a good agreement with Paul *et al.* (2006) and Sadidkhouy *et al.* (2012). In the coast of the Persian Gulf, a Moho depth of about 25 km has been suggested by Paul *et al.* (2006) where we have different values (here our estimates are around 35 km). All these comparisons between seismic estimates and regional Moho depths obtained from the different gravimetric inversion methods for each of the different sub-areas have been summarized in Table. 6.

All in all, these comparisons show that our results are in most cases in the same range with seismic estimations in literature. By considering the effects of sediment and consolidated crust we provided satisfactory results for most of the continental crust where our estimates have a relatively good agreement with local seismic studies.

Larger discrepancies are present between seismic and gravimetric estimates in the offshore area around 22 degrees of latitude. This problem has to be further investigated also following the discussion presented in Eshagh *et al.* (2017).

Table. 6. The regional seismic Moho depths in sub-areas of Iran and differences with gravimetric solutions in this area [km]

Region	Reference	Moho Depth (km)	Differences between gravimetric solutions and regional seismic Moho depths					
			Collocation		Jeffrey		Sjöberg	
			STD	RMS	STD	RMS	STD	RMS
Central Zagros	Dehghani and Makris (1984) Hatzfeld *et al.* (2003) Motaghi *et al.* (2015) Tatar and Nasrabadi (2013)	55 46 49 47	**3.2**	**3.3**	5.3	6.2	5.5	5.3
Central Alborz	Dehghani and Makris (1984) Sobouti and Arkani-Hamed (1996) Sodoudi *et al.* (2009) Radjaee *et al.* (2010) Shad Manaman *et al.* (2011) Jiménez-Munt *et al.* (2012) Taghizadeh-Farahmand *et al.* (2015)	35 45 44-46 55-58 55-60 50 54	3.5	5.6	4.2	4.3	**3.2**	**3.2**

Northwest of Iran	Nasrabadi *et al.* (2008) Taghizadeh-Farahmand *et al.* (2010) Taghizadeh-Farahmand *et al.* (2015)	40 48 41	4.8	**5.0**	4.7	9.9	**4.3**	5.9
Northeast of Iran	Dehghani and Makris (1984) Doloei and Roberts (2003) Javan Doloei and Ghafory-Ashtiany (2004) Nowrouzi *et al.* (2007) Jiménez-Munt *et al.* (2012) Taghizadeh-Farahmand *et al.* (2015)	45-48 52 52 44-50 50 45-49	**1.6**	**2.3**	2.9	6.3	1.8	5.3
Lut Block	Shad Manaman *et al.* (2011) Jiménez-Munt *et al.* (2012) Taghizadeh-Farahmand *et al.* (2015)	40 36 41	**3.0**	**7.4**	5.5	13.0	3.5	11.2
Yazd Block	Nasrabadi *et al.* (2008) Motaghi *et al.* (2015) Taghizadeh-Farahmand *et al.* (2015)	56 38 42	2.3	**8.1**	4.3	11.8	**2.2**	10.8
Central Iran	Paul *et al.* (2006) Shad Manaman *et al.* (2011) Sadidkhouy *et al.* (2012)	41 35 38.5-43	1.1	**5.3**	1.2	8.2	**0.5**	6.4
South Caspian Basin	Mangino and Priestley (1998) Shad Manaman *et al.* (2011)	30-33 30-33	10.5	**7.6**	**10.4**	**7.6**	13.9	10.9
Urumieh-Dokhtar and Sanandaj-Sirjan	Paul *et al.* (2006) Motaghi *et al.* (2015) Taghizadeh-Farahmand *et al.* (2015)	48 59 48	**6.0**	**6.1**	6.1	6.8	6.3	6.5
Oman Sea Floor and Makran	Shad Manaman *et al.* (2011) Taghizadeh-Farahmand *et al.* (2015) Abdollahi *et al.* (2018)	25-30 35 18-28	5.0	**8.2**	6.0	9.5	**4.8**	9.9
Coast of the Persian Gulf	Paul *et al.* (2006)	25	**1.6**	**3.2**	2.6	8.1	3.9	5.0

4. Summary and concluding remarks

In this study, we applied collocation method as well as two approaches based on isostasy principle presented by Sjöberg and Jeffrey for estimating the regional Moho in Iran using gravity observations. For this purpose, we considered the data of the GOCO03S satellite only global geopotential model that were subsequently reduced by topography/bathymetry, sediment and crystalline crust data effect by using the SRTM30_PLUS DTM and the CRUST1.0 model. The three different gravimetric approaches gave coherent estimates. The estimated Moho depths obtained using collocation, Jeffrey and Sjöberg's approaches proved to be statistically equivalent when compared to seismic derived values. The collocation method has been applied iteratively in three steps and the numerical computations showed that an iterative process in collocation method could not change the results significantly even though the Moho estimate based on collocation method in the third step contains more high frequency details. Furthermore, the collocation solution proved to be less biased than those based on Jeffrey and Sjöberg's methods when considering discrepancies with respect to seismic Moho estimates. To evaluate our results, we have compiled a 277 points collection of local seismic estimations in this area. The overall standard deviation of the differences between the results of the collocation, Sjöberg and Jeffrey's methods and the seismic estimates is around 6.0 km.

The minimum RMS of differences is between collocation estimates and point-wise seismic data since, as mentioned, collocation led to less biased discrepancies with the considered seismic values.

Although the application of sediment and consolidated crust corrections in our solutions provides a reasonable agreement with point-wise seismic data over most of continental areas like central Zagros, Sanandaj-Sirjan, Kopeh-Dagh and Alborz Mountains, this leads to unrealistic estimates under the Makran subduction zone, Oman Sea, Persian Gulf and Caspian Sea. This can be the effect of the poor quality of the CRUST1.0 data in this region (see Eshagh *et al.* (2017)).

The comparisons performed in this paper prove that further analyses are needed to come to a better consistency between gravity and seismic derived Moho depths in Iran before computing any joint seismic/gravimetric estimate.

References

Abbaszadeh, M., Sharifi, M. & Nikkhoo, M., 2013. A comparison of the estimated effective elastic thickness of the lithosphere using terrestrial and satellite-derived data in Iran, *Acta Geophysica,* 61**,** 638-648.

Abdollahi, S., Ardestani, V.E., Zeyen, H. & Shomali, Z.H., 2018. Crustal and upper mantle structures of Makran subduction zone, SE Iran by combined surface wave velocity analysis and gravity modeling, *Tectonophysics,* 747**,** 191-210.

Aghanabati, A., 2004. *Geology of Iran,* Geological survey of Iran.

Airy, G.B., 1855. On the computation of the effect of the attraction of mountain-masses, as disturbing the apparent astronomical latitude of stations in geodetic surveys, 145**,** 101-104.

Alavi-Naini, M., 1993. Paleozoic stratigraphy of Iran, *Treatise on the Geology of Iran,* 5**,** 1-492.

Asudeh, I., 1982. Seismic structure of Iran from surface and body wave data, *Geophysical Journal International,* 71**,** 715-730.

Bagherbandi, M. & Sjöberg, L.E., 2012. Non-isostatic effects on crustal thickness: a study using CRUST2. 0 in Fennoscandia, *Physics of the Earth Planetary Interiors,* 200**,** 37-44.

Barzaghi, A., Gandino, A., Sanso, F. & Zenucchini, C., 1992. The collocation approach to the inversion of gravity data, *Geophysical prospecting,* 40**,** 429-451.

Barzaghi, R. & Biagi, L., 2014. The collocation approach to Moho estimate, *Annals of Geophysics,* 57**,** 0190.

Barzaghi, R., Reguzzoni, M., Borghi, A., De Gaetani, C., Sampietro, D. & Marotta, A., 2015. Global to local Moho estimate based on GOCE geopotential model and local gravity data. *in VIII Hotine-Marussi Symposium on Mathematical Geodesy*, 275-282, Springer.

Bassin, C., Laske, G. & Masters, G.J.E., 2000. The current limits of resolution for surface wave tomography in North America, 81.

Becker, J., Sandwell, D., Smith, W., Braud, J., Binder, B., Depner, J., Fabre, D., Factor, J., Ingalls, S. & Kim, S., 2009. Global bathymetry and elevation data at 30 arc seconds resolution: SRTM30_PLUS, *Marine Geodesy,* 32**,** 355-371.

Beloussov, V., Belyaevsky, N., Borisov, A., Volvovsky, B., Volkovsky, I., Resvoy, D., Tal-Virsky, B., Khamrabaev, I.K., Kaila, K. & Narain, H.J.T., 1980. Structure of the lithosphere along the deep seismic sounding profile: Tien Shan—Pamirs—Karakorum—Himalayas, 70**,** 193-221.

Berberian, F., Muir, I., Pankhurst, R. & Berberian, M., 1982. Late Cretaceous and early Miocene Andean-type plutonic activity in northern Makran and Central Iran, *Journal of the Geological Society,* 139**,** 605-614.

Berberian, M. & King, G., 1981. Towards a paleogeography and tectonic evolution of Iran, *Canadian journal of earth sciences,* 18**,** 210-265.

Braitenberg, C. & Ebbing, J., 2009. New insights into the basement structure of the West Siberian Basin from forward and inverse modeling of GRACE satellite gravity data, *Journal of Geophysical Research: Solid Earth,* 114.

Braitenberg, C., Mariani, P., Reguzzoni, M. & Ussami, N., 2010. GOCE observations for detecting unknown tectonic features. *in Proc. of the ESA Living Planet Symposium*, 151-165.

Braitenberg, C., Zadro, M., Fang, J., Wang, Y. & Hsu, H., 2000. The gravity and isostatic Moho undulations in Qinghai–Tibet plateau, *Journal of Geodynamics,* 30**,** 489-505.

Dehghani, G. & Makris, J., 1984. The gravity field and crustal structure of Iran, *Neues Jahrbuch für Geologie und Paläontologie-Abhandlungen***,** 215-229.

Doloei, J. & Roberts, R., 2003. Crust and uppermost mantle structure of Tehran region from analysis of teleseismic P-waveform receiver functions, *Tectonophysics,* 364**,** 115-133.

Eftekharnezhad, J., 1980. Subdivision of Iran into different structural realms with relation to sedimentary basins (in Farsi), *Bulletin of the Iranian Petroleum Institute,* 82**,** 19-28.

Eshagh, M., Ebadi, S. & Tenzer, R., 2017. Isostatic GOCE Moho model for Iran, *Journal of Asian Earth Sciences,* 138**,** 12-24.

Eshagh, M. & Hussain, M., 2016. An approach to Moho discontinuity recovery from on-orbit GOCE data with application over Indo-Pak region, *Tectonophysics,* 690**,** 253-262.

Floberghagen, R., Fehringer, M., Lamarre, D., Muzi, D., Frommknecht, B., Steiger, C., Piñeiro, J. & Da Costa, A., 2011. Mission design, operation and exploitation of the gravity field and steady-state ocean circulation explorer mission, *Journal of Geodesy,* 85**,** 749-758.

Ghorbani, M., 2013. A summary of geology of Iran. *in The Economic Geology of Iran*, 45-64, Springer.

Gómez-Ortiz, D. & Agarwal, B.N., 2005. 3DINVER. M: a MATLAB program to invert the gravity anomaly over a 3D horizontal density interface by Parker–Oldenburg's algorithm, *Computers geosciences,* 31**,** 513-520.

Hatzfeld, D., Tatar, M., Priestley, K. & Ghafory-Ashtiany, M., 2003. Seismological constraints on the crustal structure beneath the Zagros Mountain belt (Iran), *Geophysical Journal International,* 155**,** 403-410.

Hayford, J.F., 1909. Geodesy: The Figure of the Earth and Isostasy from Measurements in the United States, *US Government Printing Office*.

Heiskanen, W., 1931. Isostatic tables for the reduction of gravimetric observations calculated on the basis of Airy's hypothesis, *Publ. Isos. Inst. IAG (Helsinki), No. 2,* 30**,** 110-153.

Heiskanen, W.A. & Moritz, H., 1967. *Physical geodesy,* edn, Vol. 86, pp. Pages, Bulletin Géodésique.

Javan Doloei, G., 2003. Transfer/Receiver Functions and its Application on Crustal Structure of Uppsala, Tehran and Mashhad Area, Ph. D Thesis, International Institute of Earthquake Engineering and Seismology (IIEES).

Javan Doloei, G. & Ghafory-Ashtiany, M., 2004. Crustal structure of Mashhad Area from time domain receiver functions analysis of teleseismic earthquake, *Research Bulletin of Seismology Earthquake Engineering***,** 30-38.

Jeffrey, H., 1976. The earth. Its origin, history and physical constitution, 6th edition, *Cambridge,* Cambridge University Press.

Jiménez-Munt, I., Fernandez, M., Saura, E., Vergés, J. & García-Castellanos, D., 2012. 3-D lithospheric structure and regional/residual Bouguer anomalies in the Arabia—Eurasia collision (Iran), *Geophysical Journal International,* 190**,** 1311-1324.

Krarup, T., 1969. A contribution to the mathematical foundation of physical geodesy, *Geod. Inst. Copenhagen, Medd.,* 44.

Laske, G., Masters, G., Ma, Z. & Pasyanos, M., 2013. Update on CRUST1. 0—A 1-degree global model of Earth's crust. *in Geophys. Res. Abstr*, pp. 2658EGU General Assembly Vienna, Austria.

Mangino, S. & Priestley, K., 1998. The crustal structure of the southern Caspian region, *Geophysical Journal International,* 133**,** 630-648.

Mayer-Gürr, T., Rieser, D., Höck, E., Schuh, W.-D., Krasbutter, I., Kusche, J., Maier, A., Krauss, S., Hausleitner, W. & Baur, O., 2012. The new combined satellite only model GOCO03S. *in GGHS2012, Venice*.

Mooney, W.D., Laske, G. & Masters, T.G.J.J.o.G.R.S.E., 1998. CRUST 5.1: A global crustal model at 5× 5, 103**,** 727-747.

Moritz, H., 1980. Advanced physical geodesy, *Advances in Planetary Geology*.

Moritz, H., 1990. The figure of the Earth, *Wichmann, Karlsruhe,* 353.

Motaghi, K., Tatar, M., Priestley, K., Romanelli, F., Doglioni, C. & Panza, G., 2015. The deep structure of the Iranian Plateau, *Gondwana Research,* 28**,** 407-418.

Nabavi, M., 1976. History of Iran Geology, *Geological Survey Mineral Exploration Country*.

Nasrabadi, A., Tatar, M., Priestley, K. & Sepahvand, M., 2008. Continental lithosphere structure beneath the Iranian plateau, from analysis of receiver functions and surface waves dispersion. *In 14th World Conference on Earthquake Engineering*, 17.

Nowrouzi, G., Priestley, K.F., Ghafory-Ashtiany, M., Doloei, G.J. & Rham, D.J., 2007. Crustal velocity structure in Iranian Kopeh-Dagh, from analysis of P-waveform receiver functions, *Journal of Seismology Earthquake Engineering,* 8**,** 187-194.

Oldenburg, D.W., 1974. The inversion and interpretation of gravity anomalies, *Geophysics,* 39**,** 526-536.

Parker, R., 1973. The rapid calculation of potential anomalies, *Geophysical Journal of the Royal Astronomical Society,* 31**,** 447-455.

Paul, A., Kaviani, A., Hatzfeld, D., Vergne, J. & Mokhtari, M., 2006. Seismological evidence for crustal-scale thrusting in the Zagros mountain belt (Iran), *Geophysical Journal International,* 166**,** 227-237.

Pratt, J., 1855. On the attraction of the Himalaya Mountains, and of the elevated regions beyond them, upon the plumb-line in India, 145**,** 53-100.

Radjaee, A., Rham, D., Mokhtari, M., Tatar, M., Priestley, K. & Hatzfeld, D., 2010. Variation of Moho depth in the central part of the Alborz Mountains, northern Iran, *Geophysical Journal International,* 181**,** 173-184.

Reguzzoni, M., Sampietro, D. & Sansò, F., 2013. Global Moho from the combination of the CRUST2. 0 model and GOCE data, *Geophysical Journal International,* 195**,** 222-237.

Sadidkhouy, A., Alikhani, Z. & Sodoudi, F., 2012. The variation of Moho depth and V P/V S ratio beneath Isfahan region, using analysis of teleseismic receiver function, *Journal of the Earth space Physics,* 38**,** 15-24.

Sampietro, D., 2011. GOCE exploitation for Moho modeling and applications. *In Proceedings of the 4th international GOCE user workshop*.

Sampietro, D., 2016. Crustal modelling and Moho estimation with GOCE gravity data. *In Remote sensing advances for earth system science*, 127-144, Springer.

Sampietro, D., Reguzzoni, M. & Braitenberg, C., 2014. The GOCE estimated Moho beneath the Tibetan Plateau and Himalaya. *In Earth on the Edge: Science for a Sustainable Planet*, 391-397, Springer.

Shad Manaman, N., Shomali, H. & Koyi, H., 2011. New constraints on upper-mantle S-velocity structure and crustal thickness of the Iranian plateau using partitioned waveform inversion, *Geophysical Journal International,* 184**,** 247-267.

Shin, Y.H., Xu, H., Braitenberg, C., Fang, J. & Wang, Y., 2007. Moho undulations beneath Tibet from GRACE-integrated gravity data, *Geophysical Journal International,* 170**,** 971-985.

Sjöberg, L.E., 2009. Solving Vening Meinesz-Moritz inverse problem in isostasy, *Geophysical Journal International,* 179**,** 1527-1536.

Sobouti, F. & Arkani-Hamed, J., 1996. Numerical modelling of the deformation of the Iranian plateau, *Geophysical Journal International,* 126**,** 805-818.

Sodoudi, F., Yuan, X., Kind, R., Heit, B. & Sadidkhouy, A., 2009. Evidence for a missing crustal root and a thin lithosphere beneath the Central Alborz by receiver function studies, *Geophysical Journal International,* 177**,** 733-742.

Taghizadeh-Farahmand, F., Afsari, N. & Sodoudi, F., 2015. Crustal thickness of Iran inferred from converted waves, *Pure Applied Geophysics,* 172**,** 309-331.

Taghizadeh-Farahmand, F., Sodoudi, F., Afsari, N. & Ghassemi, M.R., 2010. Lithospheric structure of NW Iran from P and S receiver functions, *Journal of Seismology,* 14**,** 823-836.

Tapley, B.D., Bettadpur, S., Ries, J.C., Thompson, P.F. & Watkins, M.M., 2004a. GRACE measurements of mass variability in the Earth system. *In Science*, 503-505.

Tapley, B.D., Bettadpur, S., Watkins, M. & Reigber, C., 2004b. The gravity recovery and climate experiment: Mission overview and early results. *In Geophysical Research Letters*.

Tatar, M. & Nasrabadi, A., 2013. Crustal thickness variations in the Zagros continental collision zone (Iran) from joint inversion of receiver functions and surface wave dispersion, *Journal of seismology,* 17**,** 1321-1337.

Tenzer, R., Hamayun, K. & Vajda, P., 2009. Global maps of the CRUST 2.0 crustal components stripped gravity disturbances, *Journal of Geophysical Research: Solid Earth,* 114.

Tenzer, R., Novák, P. & Gladkikh, V., 2011. On the accuracy of the bathymetry-generated gravitational field quantities for a depth-dependent seawater density distribution, *Studia Geophysica et Geodaetica,* 55**,** 609.

Tenzer, R., Novák, P., Gladkikh, V. & Vajda, P., 2012a. Global crust-mantle density contrast estimated from EGM2008, DTM2008, CRUST2. 0, and ICE-5G, *Pure applied geophysics,* 169**,** 1663-1678.

Tenzer, R., Pavel, N. & Vladislav, G., 2012b. The bathymetric stripping corrections to gravity field quantities for a depth-dependent model of seawater density, *Marine Geodesy,* 35**,** 198-220.

Tscherning, C., 1985. Local approximation of the gravity potential by least squares collocation, *Proc, Int. Summer School on Local Gravity Field Approximation***,** 277-362.

Vening Meinesz, F.A., 1931. Une nouvelle methode pour la reduction isostatique regionale de l'intensite de la pesanteur, *Bulletin geodesique,* 29**,** 33-51.
Watts, A.B., 2001. *Isostasy and Flexure of the Lithosphere*, Cambridge University Press.